ACS OMEGA

Open Access

http://pubs.acs.org/journal/acsodf

Article

Flooding Performance and Optimization of Injection Parameters of Nanosized Oil Displacement Agents in Extra-Low-Permeability Reservoirs

Zhiying Deng,* Zhiwei Li, Peng Li, Wenchao Wu, Liwei Xiong, Zhanhui Zhang, Yuxi Yang, and Youyou Cheng

Cite This: *ACS Omega* 2024, 9, 19043−19050

Read Online

ACCESS | Metrics & More | Article Recommendations

ABSTRACT: There have been few studies on the role of nanofluids in oil displacement and injection parameters, despite their significant impact on the oil displacement effect. To enhance oil recovery in an ultralow-permeability reservoir, the nanosized oil-displacement agent with nano-SiO_2 modified by a silane coupling agent as a main component was selected for the first time in the Changqing oilfield. To assess the performance of the nanofluid, various factors such as particle size, contact angle, interfacial tension, and emulsion stability were taken into consideration. The oil displacement effect of nanofluids was evaluated by a microscopic model and ultralow-permeability core displacement experiment, and its optimal injection parameters were determined. The average particle size of the nano-oil displacement agent is 22−30 nm. It can change the wetting condition of the rock from oil-wet to water-wet and reduce the oil−water interfacial tension. Even at 80 °C, the emulsion formed by the agent remained stable. The oil displacement experiment shows that the nano-oil displacement agent whose injection pressure increases can displace the residual oil trapped in small pores that cannot be affected by conventional water flooding. The injection mode of "nanoflooding agent drive + water drive + nanoflooding agent drive", injection rate of 0.1 mL/min, injection concentration of 0.5%, and injection volume of 0.5 PV (0.25 PV per segment), which can effectively guide the injection of the oil displacement agent, achieve the best oil displacement effect.

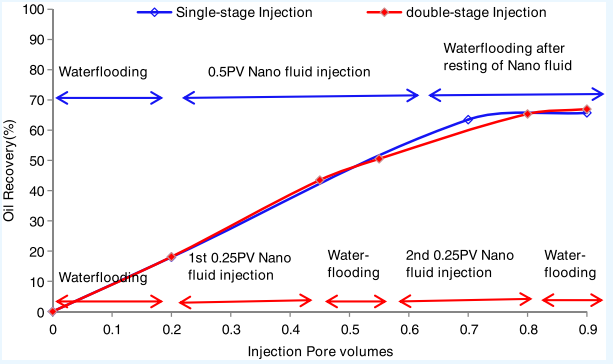

1. INTRODUCTION

With the reduction of conventional hydrocarbon resources in medium/high-permeability reservoirs and the progress of petroleum exploration and development technology, low-permeability reservoir hydrocarbon resources gradually replace conventional oil and gas and become the focus of oilfield development.[1−3] Low-permeability oil and gas resources in China are rich in reserves and are mainly developed by water injection. Many problems include high injection pressure, low recovery, and a poor oil displacement effect.[4,5] The Chang 8 reservoir in Ordos Basin is taken as an example, which belongs to the sedimentary environment of the shallow water area of the Delta Front subfacies lake, with multibranch channel crisscrossing, rapid lateral change of the sand body, strong diagenetic compaction and cementation in the later stage, and is a lithologic reservoir, with the feldspar content high (60%) and particle size (median of 30 μm) and pore roar (radius of 0.12 μm) smaller, and so on. The production of the waterflood development reservoir accounts for 92.2%, among which extra-low permeability (average permeability of 10−1 mD) accounts for 32.5% and ultralow permeability (average permeability of <1 mD) accounts for 34.7%. The current geological recovery degree is 8.6%, far less than the recoverable recovery degree (44.9%).[6]

Bernard et al.[7] found that the replacement of clay-bearing sandstone cores with low-mineralization NaCl brine increased the oil recovery. In addition to the fact that the mechanism of oil drive in low-mineralization water drives is not clear, there are also water source problems and reservoir adaptability issues. To improve the recovery efficiency of low-permeability reservoirs, researchers actively explore the injection of the surfactant, microemulsion, microsphere, and other methods, but there are some problems with the existing liquid system. Researchers found that some surfactants have the ability for

Received: December 4, 2023
Revised: March 10, 2024
Accepted: March 14, 2024
Published: April 18, 2024

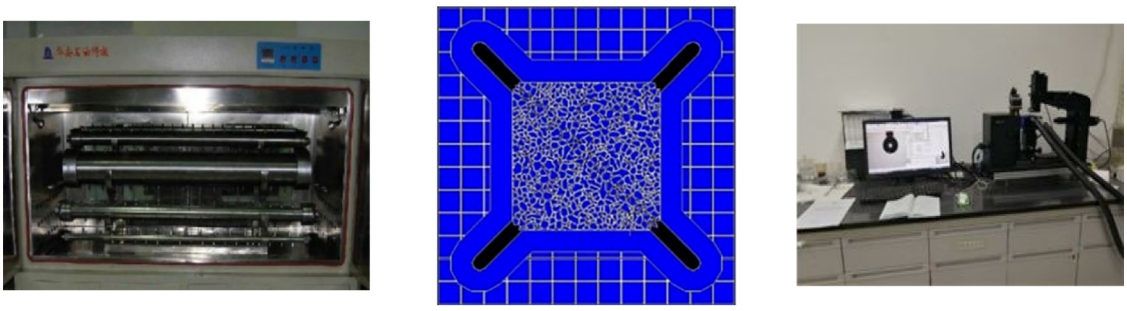

(a) Sand pack model photo (b) Microchip physical model photo (c) Contact angle measuring instrument

Figure 1. (a) Sand pack model, (b) microchip physical model photo, and (c) contact angle measuring instrument (Photo provided by Wu Wenchao. Copyright 2023−2024. The images in this article are free).

wet reversal, but the low-permeability reservoir has a large surface area, a large amount of surfactant injection, a long operation cycle, high cost, and difficulty in field implementation.[8] With the advent of nanotechnology, nanofluids have been applied to oilfield development. The experimental results from Wei et al. are reported.[9] They show that nanoparticles can change wettability, reduce oil−water interfacial tension, produce wedge-shaped permeability, and so on, to enhance the recovery efficiency.[10,11] Among the numerous nanoparticles, SiO_2 nanoparticles have the advantages of convenient acquisition, low price, easy modification, and adjustable size, which have the potential to achieve large-scale production and application. At present, researchers mainly focus on the development and performance evaluation of nano-oil displacement agents, but the role of nanofluids in oil displacement, injection timing, and injection parameters is less studied. The injection time, injection rate, injection amount, and injection method of the SiO2 nanofluid greatly influence the oil displacement effect in ultralow-permeability reservoirs.[12−16] Taborda et al.[17] had a primary objective—the evaluation of the effect of surface acidity of silica nanoparticles for mitigation of time-dependent thermal degradation of polymer solutions of partially hydrolyzed polyacrylamide (HPAM), for employment in chemical enhanced oil recovery (EOR) processes. Hassan et al.[18] synthesized and characterized a new ZnOFe2O3/SiO2 nanohybrid for the preparation of the ZnOFe2O3/SiO2-based nanofluid. The EM-driven approach of tuning the EOR technique is significant to improve the NP mobility in the reservoir. In the study of Yekeen et al.,[19] a natural surfactant, saponin, was isolated from soapnut (Sapindus Mukorossi) and the extracted saponin could be considered a supplementary alternative to conventional EOR surfactants.

This paper first evaluated the basic performance of the nanodisplacement agent, then studied the flow characteristics and displacement characteristics of the nanodisplacement agent through microscopic model displacement experiments, and finally evaluated the displacement effect of the nanodisplacement agent from the two aspects of pressure change and enhanced oil recovery. The effects of injection timing, injection volume, injection rate, injection concentration, and injection method on the EOR were studied, and the injection parameters were determined to make the best effect of the nano-oil displacement agent, which provides guidance for the later application of the oilfield.

2. EXPERIMENTS

2.1. Materials and Equipment. Experimental materials: crude oil, L1 Chang 8 reservoir of Changqing Oilfield; Kerosene, Wuhan Xiang He Yi Chemical Technology Co., Ltd; simulated crude oil (crude oil: kerosene = 1:2), surface tension of 24 mN/m; simulated formation water (salinity of 20,000 mg/L, KCl: 310 mg/kg, $MgCl_2$: 3480 mg/kg, Na_2SO_4: 1380 mg/kg, NaCl: 12,830 mg/kg, $CaCl_2$: 430 mg/kg, Na_2CO_3: 1570 mg/kg), surface tension of 72 mN/m; and nano-oil displacement agent, nano-SiO2 material synthesized with vinyl trimethoxysilane as a coupling agent, Xi 'an Changqing Chemical Group Co., Ltd, the effective content of nano-oil displacement agent mother liquid (ML) was 20.68%, the surface tension of 0.5% nano-oil displacement agent was 62 mN/m, and the nanoflooding system with different concentrations was prepared by using simulated formation water.

Equipment: sand pack model (150 mesh quartz sand-filled and compacted, permeability between 1 and 10mD); Microchip physical model (see Figure 1, aperture = 3−5 μm, length × width = 76 mm × 76 mm, thickness = 3.6 mm), permeability 1−10mD, Zhenjiang Huarui Chip Technology Co., Ltd; CCD microscope, Longji Instrument Equipment Co; Omni multiangle particle size and high-sensitivity zeta potential analyzer, Brookhaven Instruments; JJ2000B rotary drop interface tensimeter and JJ2000B contact angle meter, Shanghai Zhongchen Digital Technology Equipment Co., Ltd; and field emission scanning electron microscope, FEI Czech., Ltd.

2.2. Experimental Methods. *2.2.1. Evaluation of Basic Properties of the Nano-Oil Displacement Agent.* (1) Particle size distribution: at 80 °C, the particle size distribution curves of nano-oil displacement agents with different concentrations were measured by a laser Omni multiangle particle size analyzer. (2) Stability: refer to the GB/T 32668−2016 General Principles of Colloid Particle ζ Potential Analysis electrophoresis. (3) Interfacial tension: Refer to the SY/T5370−1999 surface and interfacial tension determination method. The steady-state interfacial tension between the nano-oil displacement agent and crude oil with different concentrations was measured at 80 °C and 7500 r/min using a rotary drop interfacial tensiometer. (4) Wettability: At room temperature, the simulated core slice was made by a quartz sand pressing tablet, which was immersed in a nanoaqueous solution with different concentrations for 1 h. The contact angle of the nano-oil displacement agent with different concentrations was determined according to the SY/T5153−2007 Reservoir rock wettability determination method.

https://doi.org/10.1021/acsomega.3c07863
ACS Omega 2024, 9, 19043−19050

2.2.2. Microscopic Model Displacement Effect. First, simulated crude oil was injected into the microchip physical mode at a rate of 0.2 mL/min at room temperature. Second, the simulated formation water drove the simulated oil in the chip at a rate of 0.1 mL/min until no more oil was produced. Then, 0.5% nano-oil displacement agent was used for displacement. During displacement, a CCD microscope was used to photograph the effect of oil displacement in the microchannel. Finally, it was washed with kerosene after the experiment.

2.2.3. Injection Parameter Optimization. At 80 °C, referenced to the SY/T5336−2006 ≪Method for Determination of Relative Permeability of Two-phase Fluid in Rock≫, the core displacement experiment was carried out. Experimental procedures for parameter optimization of injection concentration and injection rate: (circled 1) dry sand filling tube and sand, the dry weight of the sand filling tube, dry weight of "sand + sand filling tube", and wet weight of saturated sand + sand filling tube. (Circled 2) The initial oil saturation was calculated when the oil displacement water reached 98% of the oil produced. (Circled 3) Water drove to 50% recovery. (Circled 4) The nano-oil displacement agent was used for oil displacement. The injection rate and injection mode of experimental steps (circled 1) and (circled 2) were the same as above; step (3) optimized the oil displacement sequence according to the injection volume and injection method, and the experimental pressure was recorded throughout the experiment from step (3). The injection concentration of the nano-oil displacement agent was 0.1, 0.5, and 1.0%. Injection rates were 1.0, 1.5, and 2.0 mL/min, respectively. The injection amounts were 0.2 PV water + 0.5 PV nano-oil displacement agent, 0.3 PV water + 0.4 PV nano-oil displacement agent, 0.4 PV water + 0.3 PV nano-oil displacement agent, and 0.5 PV water + 0.2 PV nano-oil displacement agent. The injection modes were two-stage injection mode (0.2 PV water + 0.25 PV nano-oil displacement agent + 0.1 PV water + 0.25 PV nano-oil displacement agent + 0.1 PV water) and single-stage injection mode (0.2 PV water + 0.5 PV nano-oil displacement agent + 0.2PV water)

2.2.4. Scanning Electron Microscopy (SEM) Test of Quartz Sand before and after Displacement. The sand-filled tube model was replaced with 0.5% nano-oil displacement agent for 10 days, and quartz sand was recovered. Then, SEM was used to scan the quartz sand before displacement and the quartz sand near the inlet and outlet of the sand filling pipe for analysis of the adsorption characteristics of the nano-oil displacement agent in the process of displacement.

3. EXPERIMENTAL RESULTS AND DISCUSSION

3.1. Evaluation of Basic Properties of the Nano-Oil Displacement Agent. *3.1.1. Particle Size Distribution.* The particle size distribution curve of the nano-oil displacement agent is shown in Figure 2. At 80 °C, the particle size range of nanoflooding systems with different concentrations is slightly different. With the increase of the concentration of the nanoflooding system, the average particle size distribution range increased but was still mainly 10−100 nm, and the average particle size was 22−30 nm, which showed that the modified nano-SiO_2 particles in the nano-oil displacement agent have a smaller particle size, which is favorable to spread to nanoscale pores.

3.1.2. Stability. The higher the absolute value of the ζ potential of the system, the more stable the system was. In the aqueous phase, the stability boundary of the system was generally ±30 mV. If the absolute value of the ζ potential of all particles was higher than 30 mV, the system was stable. Figure 3 shows that the surface of nano-oil displacement agent SiO2 particles was negatively charged. When the concentration increased from 0.1 to 0.5%, the ζ potential increased from −46.28 to −32.50 mV, and the absolute value of the ζ-potential was still higher than 30 mV, but the absolute value decreased, the ζ-potential of mother liquid (pure nano-oil displacement agent solution) dropped to −29.74 mV, and the solution became less stable. This was because the silicon dioxide was modified by introducing several modified groups, which made ions in formation water associated with the nano-oil flooding system and occupied the adsorption layer and diffusion layer, resulting in an abnormal trend of ζ potential. At the same time, because of the high concentration of nanoparticles in the nanoflooding agent, the spacing between particles decreased, the probability and frequency of collision and aggregation increased, the interaction between them increased, and the convergence occurred, which made the system less stable. Therefore, the concentration of the nanodisplacement agent should not be too high; when the concentration was lower than 0.5%, the system had good stability.

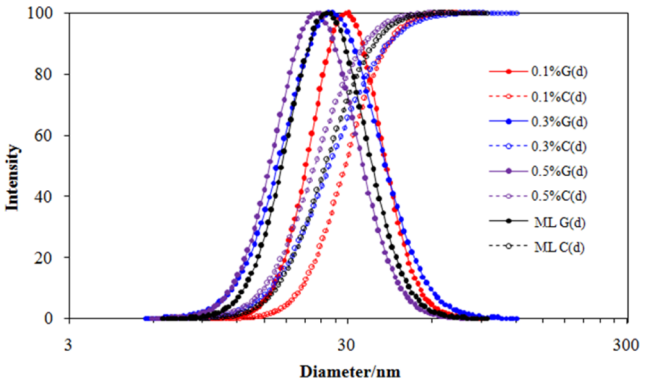

Figure 2. Microscopic particle size distribution of the nano-oil displacement agent. G(d) is the ratio of individual particle size to average particle size and C(d) is the ratio of individual particle size to cumulative particle size.

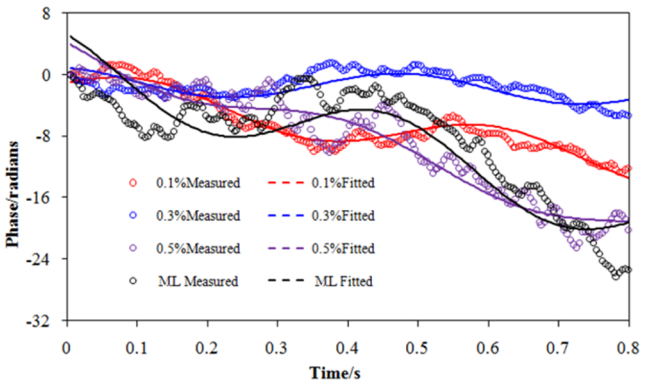

Figure 3. ζ Potential test chart.

3.1.3. Interfacial Tension. As can be seen from Figure 4a, the interfacial tension between the nanoflooding system and the crude oil in the test area approximately reached equilibrium at a constant temperature (80 °C) within about 10 min and

https://doi.org/10.1021/acsomega.3c07863
ACS Omega 2024, 9, 19043−19050

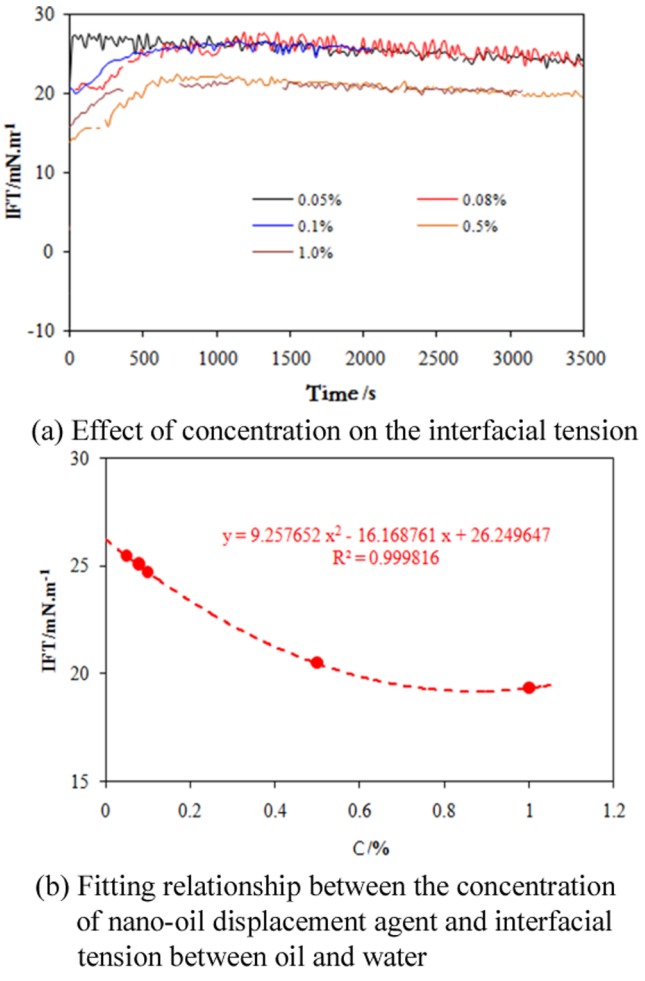

Figure 4. Relationship between interfacial tension and concentration of the nano-oil displacement agent under reservoir conditions.

remained stable. The oil−water interfacial tension decreased with the increase of the concentration of the nano-oil flooding system, but it was still mainly distributed between 19 and 25 mN/m. The nano-oil displacement system can reduce the oil−water interfacial tension. The reduction of interfacial tension from 0.5 to 0.1% was 14.12%, much greater than that from 1.0 to 0.5%, which was 3.85%. In addition, according to the fitting curve of concentration and interfacial tension of the nano-flooding system (Figure 4b), the calculated interfacial tension was about 22.23 mN/m when the concentration of the nanoflooding system was 0.3%, which was about 8.23% lower than that when the concentration of nanoflooding system was 0.1%. When the concentration range of the nano-oil flooding system was 0.3−0.5%, it was beneficial to peel off the crude oil adsorbed on the pore surface and reduced the work of small oil droplets through the small pores due to deformation, so that the crude oil was more easily displaced from the small pores to the pore throat, which was good for the enhanced oil recovery.[20]

3.1.4. Wettability. At room temperature, the wetting contact angles of mother liquor and 0.1, 0.5, 1.0, and 1.5% nano-oil displacement agent on the quartz sand tablet were 75.9, 66.8, 61.5, 59.8, and 58.2°, respectively (see Figure 5). With the increase of the concentration, the contact angle became smaller, and the hydrophilicity became stronger, which was conducive to stripping oil from the rock surface. Figure 6

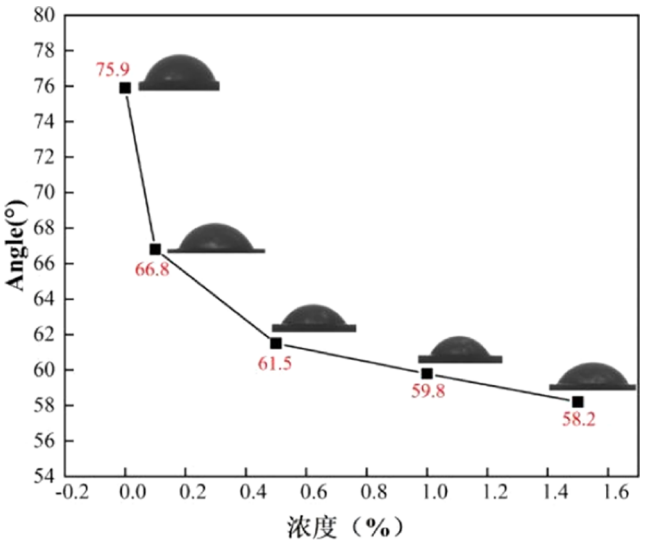

Figure 5. Effect of nano-oil displacement agent concentration on the contact angle.

shows the situation before and after the adsorption of the nano-oil flooding agent on the quartz sand surface. From Figure 6a, it can be seen that the nanoparticles of the nano-oil displacement agent solution are spherical and uniformly dispersed, there were vacuums in the middle, and there may be large branched chains in the structure. As can be seen from Figure 6b, the surface of quartz sand without the nanoflooding agent is smooth and clean, while the surface of quartz sand is nail type after it adsorbs the nano-oil displacement agent, which indicated that the nano-oil displacement agent was separated from the residual inorganic salt ions on the surface of the quartz sand platen during the adsorption process, thus releasing the hydrophilic nanosilicon dioxide nucleus; it was beneficial to adsorb on the surface of sandstone and then changed its wettability to form a more hydrophilic surface.[21,22] It can be seen that the nano-oil displacement agent can be adsorbed on the rock, change the wettability of the rock layer, reduce the contact angle of water droplets, and enhance the hydrophilicity of the rock surface to make the oil layer in the core fall off faster and achieve the purpose of displacement.

3.2. Oil Displacement Effect of the Nano-Oil Displacement Agent Microscopic Model. In the microscopic model, the microchip channel was filled with simulated crude oil; then, a water flooding experiment was carried out to make the microscopic model reach the state of residual oil; at the same time, a CCD microscope (magnification 98) was used to record the simulated oil distribution before and after the water drive (see Figure 7a). The residual oil in the curved flaky throat had little change after the water drive until the simulated oil did not move, which was mainly the trapped oil in the small pores and the oil adsorbed on the pore surface, distributed in a network pattern[23] (see Figure 7b). Finally, with the use of a nano-oil displacement agent, the remaining oil in the pore significantly reduced, and the remaining residual oil remained in smaller pores (see Figure 6c). It can be seen that nano-oil displacement agents can spread to the small pores that were not affected by the conventional water drive, thus increasing the oil displacement efficiency. In addition, after water flooding was replaced by a nano-oil displacement agent, the injection pressure increased significantly (see Figure 8), and the swept area increased, thus enhancing oil recovery.

https://doi.org/10.1021/acsomega.3c07863
ACS Omega 2024, 9, 19043−19050

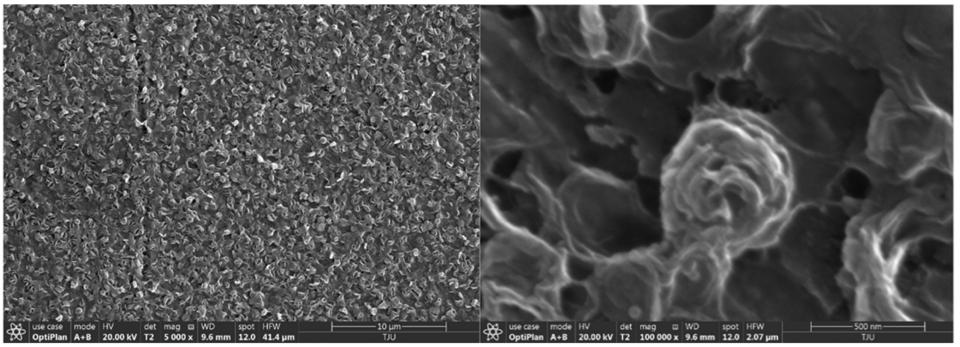

(a) Sem image of pure nano-oil displacement agent solution

(b) Sem images before and after adsorption of nanoparticles by quartz sand compression

Figure 6. Scanning electron microscopy image of the nano-oil displacement agent.

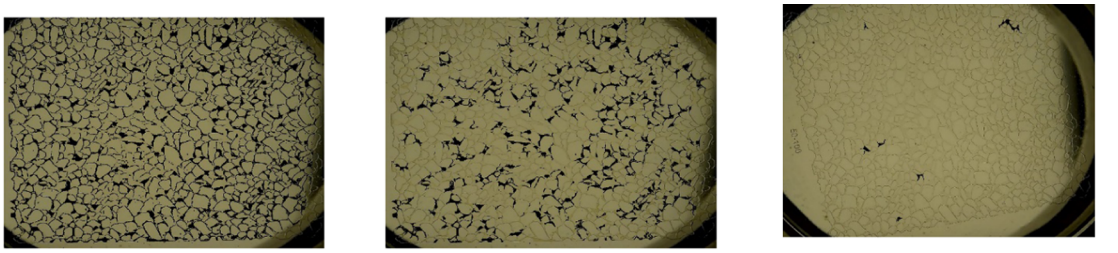

(a)Microchip saturated oil profile before displacement

(b) Residual oil distribution after water drive

(c) Residual oil distribution after 0.5% nano oil displacement agent

Figure 7. Changes in the core oil displacement experiment

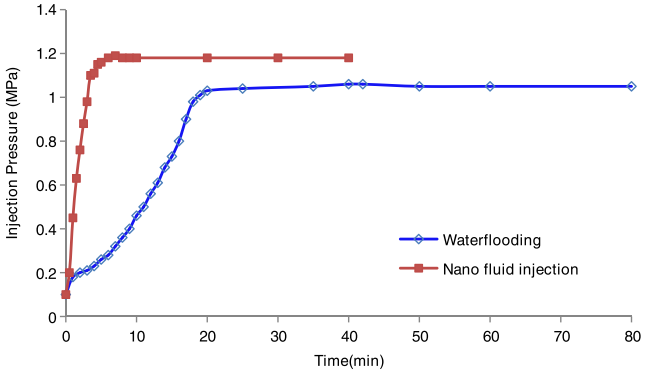

Figure 8. Pressure curve at the injection end.

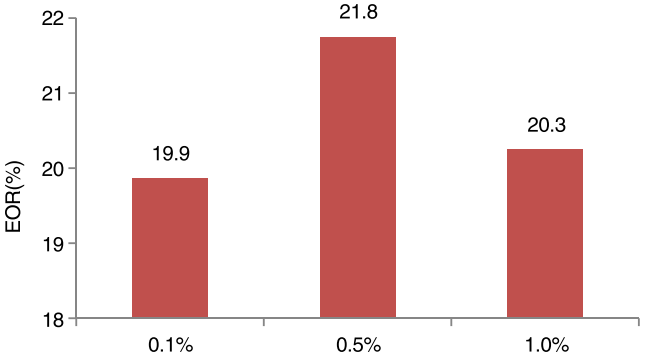

Figure 9. Oil displacement effect under different concentrations of the nano-oil displacement agent.

3.3. Optimization of Injection Parameters. *3.3.1. Injection Concentration.* The influence of the nano-oil displacement agent on the EOR under different concentrations at an injection rate of 0.1 mL/min and an injection volume of 0.3 PV on injection pressure is shown in Figure 9. With increasing injection concentration, the recovery efficiency first increased and then decreased (Figure 9). When the concentration of the nano-oil displacement agent was 0.5%, the EOR was greatly enhanced (21.8%), and the final recovery efficiency became 71.8% because excess nano-oil displacement agent was

https://doi.org/10.1021/acsomega.3c07863
ACS Omega 2024, 9, 19043−19050

adsorbed on the rock surface when the concentration of the nano-oil displacement agent was higher than 0.5%, which made the seepage channels smaller and reduced oil recovery efficiency.[24] The optimal concentration of the nano-oil displacement agent was 0.5%.

3.3.2. Injection Rate. The effect of the injection rate of 0.5% nano-oil displacement agent with an injection rate of 0.5 PV on the EOR at different injection rates is shown in Figure 10. At

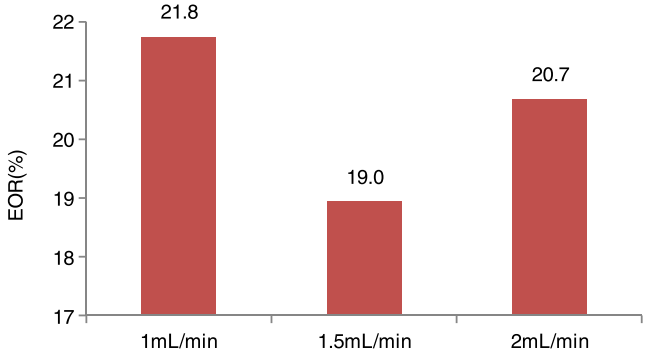

Figure 10. Displacement effect under different injection rates.

the injection rate of 1.0 mL/min, the oil recovery was enhanced by 21.8%, and the final recovery was 71.8%. In addition, the higher the injection rate was, the worse the effect of the EOR was. This phenomenon could be attributed to the limited pore volume of the laboratory core. An increase in the injection rate increased the migration rate of the nano-oil displacement agent with the fluid and shortened the contact time between the oil displacement agent and the rock wall. The increase in the injection was not favorable to the nano-oil displacement agent adsorption on the rock surface, causing the oil to flow out in a short time, forming a flow channel and leading to the fingering phenomenon. Thus, the subsequent displacement fluid mainly moved along the flow channel, and the remaining oil in the surrounding pores could not be displaced, reducing recovery efficiency. The optimal injection rate of the nano-oil displacement agent was 1.0 mL/min.

3.3.3. Injection Volume. The effect of the nano-oil displacement agent on the EOR at different injection volumes is shown in Figure 11. The recovery rate was the highest (62.3%) when the injection amount of the nano-oil displacement agent was 0.5 PV at the same total injection amount of water and the nanoflooding agent. With decreasing nano-oil displacement agent injection amount, the total recovery rate

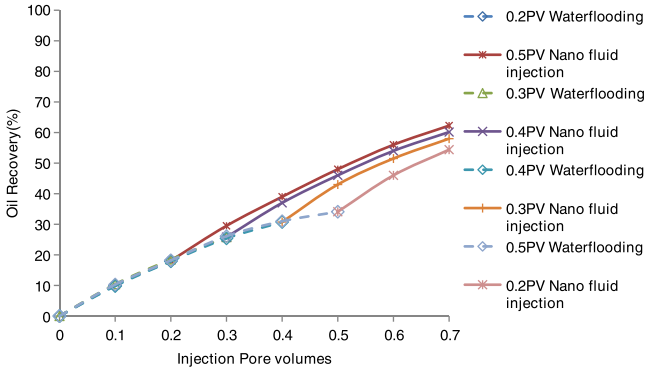

Figure 11. Displacement effect under different injection volumes.

decreased and the oil displacement effect gradually deteriorated. The average water injection pressure increased from 0.16 to 0.25 MPA after four groups of water flooding were changed to nano-oil displacement agents. The increase in injection pressure indicated that the nano-oil displacement agent could effectively enhance the oil recovery rate. The optimal injection volume of the nano-oil displacement agent was 0.5 PV.

3.3.4. Injection Mode. Figure 12 shows the influence of the nano-oil displacement agent on the EOR under different

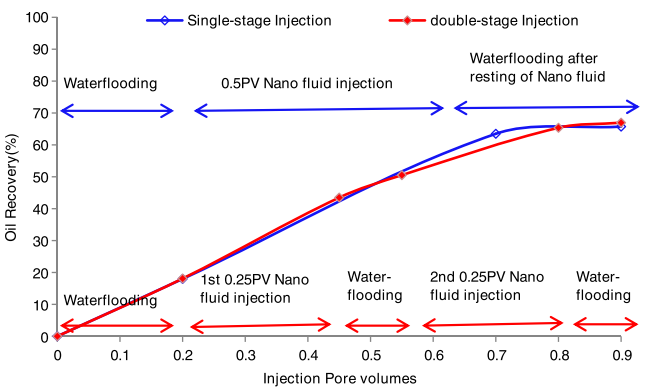

Figure 12. Different injection methods for the ultralow-permeability model.

injection methods and optimal conditions, with an injection rate of 1.0 mL/min and injection volume of 0.5 PV. Figure 12 shows that two-stage injection (0.2 PV water + 0.25 PV nanoflooding agent + 0.1 PV water + 0.25 PV nanoflooding agent + 0.1 PV water) achieved 67.0% recovery, which was better than that of single-stage injection (0.2 PV water + 0.5 PV nanoflooding agent + 0.2 PV water) (66.7%). This improved recovery rate was because the two-stage injection method divided the 0.5 PV nanoflooding agent into two 0.25 PV injections, with 0.1 PV water in between. This process increased the retention time of the nanoflooding agent in the core, which gave more time for the displacement agent to pull the oil out of the micropores from other pores, thus improving the recovery.

3.4. SEM Test of Quartz Sand before and after Displacement. As shown in Figure 13, the quartz sand surface was smooth with a few grains protruding before displacement (Figure 13a), a layer of spherical particles was attached to the quartz sand surface at the entrance after displacement (Figure 13b), and a considerable accumulation of particles and multilayer adsorption of nanoparticles were observed at the exit (Figure 13c). This showed that nanoparticles of the oil displacement agent could be adsorbed on the rock surface to change the wettability of the rock. The adsorption capacity at the outlet was much higher than that at the inlet. The higher adsorption indicated that the nano-oil displacement agent had a good migration rate with a hydrophobic slippage effect and could enter deep strata, and the adsorption amount increased in the process of migration in the core. Therefore, the purpose of expanding sweep volume was achieved.

4. CONCLUSIONS

To enhance oil recovery in an ultralow-permeability reservoir, the selection of a nanosized oil-displacement agent with nano-SiO_2 modified by a silane coupling agent as a primary

https://doi.org/10.1021/acsomega.3c07863
ACS Omega 2024, 9, 19043−19050

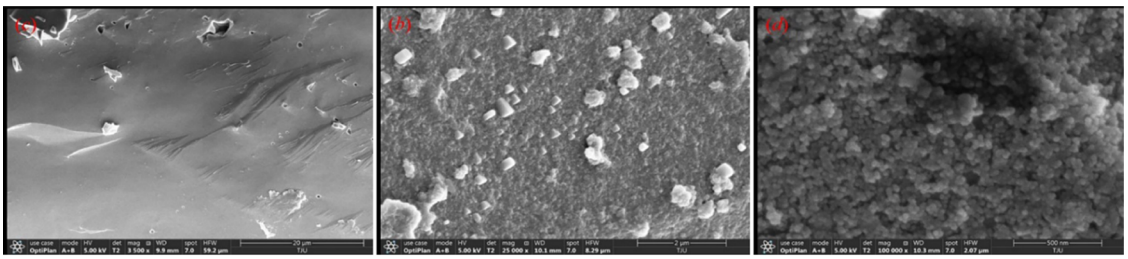

(a) Pre-displacement blank quartz sand (b) Post-displacement inlet quartz sand (c) Export quartz sand after displacement

Figure 13. SEM images of quartz sand before and after core displacement with the nano-oil displacement agent.

component has been introduced for the first time in Changqing Oilfield. Based on the performance evaluation, microscopic model tests, and ultralow-permeability core displacement experiment, the following key findings have been drawn.

(1) The nano-oil displacement agent, characterized by an average particle size of 22−30 nm, absolute ζ potential above 30 mV, interface tension of 22.23 mN/m, and EOR increased by about 20%, features a negatively charged surface, ensuring system stability, low interfacial tension, and excellent hydrophilicity.
(2) Compared with water flooding, the nano-oil flooding system increases injection pressure and exhibits superior displacement effectiveness in curved and flaked throats, making it well-suited for capturing residual oil in small pores that conventional water flooding cannot affect, thus improving oil displacement efficiency.
(3) The recommended injection mode for the nano-oil displacement agent in the special permeability reservoir of the Changqing oilfield is the injection method of "water flooding + nano-oil flooding + water flooding + nano-oil flooding + water flooding". The optimal injection parameters include an injection rate of 0.1 mL/min, an injection concentration of 0.5%, and a nano-oil displacement agent injection volume of 0.5 PV, with each section receiving 0.25 PV.
(4) The nano-oil displacement agent demonstrates excellent mobility and deep adsorption within the formation, thereby enlarging sweep volume during the core migration process.
(5) Although significant progress has been achieved in the research and experimentation of nano-oil displacement agents, the focus has remained primarily on injection parameters and EOR effects. Limited attention has been given to the mechanisms of injection timing and sweep volume expansion. To address this gap, future efforts should concentrate on a well-balanced combination of laboratory research and field requirements.

■ ASSOCIATED CONTENT

Data Availability Statement

The data used to support the findings of this study are included in the article.

■ AUTHOR INFORMATION

Corresponding Author

Zhiying Deng − *Hubei Key Laboratory of Plasma Chemistry and Advanced Materials, Wuhan Institute of Technology, Wuhan 430205, P. R. China; National Engineering Laboratory for Exploration and Development of Low-Permeability Oil and Gas Field, Xi'an 710018, P. R. China; Oil & Gas Technology Research Institute of Changqing Oil Field Company, Xi'an 710018, P. R. China*; Email: 659464170@qq.com

Authors

Zhiwei Li − *The Fourth Oil Production Plant of Changqing Oil Field Company, Xi'an 710018, P. R. China*

Peng Li − *The Fourth Oil Production Plant of Changqing Oil Field Company, Xi'an 710018, P. R. China*

Wenchao Wu − *Shanxi Ming De Petroleum Technology Limited Company, Xi'an 710018, P. R. China*

Liwei Xiong − *Hubei Key Laboratory of Plasma Chemistry and Advanced Materials, Wuhan Institute of Technology, Wuhan 430205, P. R. China*

Zhanhui Zhang − *Hubei Key Laboratory of Plasma Chemistry and Advanced Materials, Wuhan Institute of Technology, Wuhan 430205, P. R. China*

Yuxi Yang − *School of Earth Science and Engineering, Xi'an Shiyou University, Xi'an 710065, P. R. China*; orcid.org/0009-0004-4378-827X

Youyou Cheng − *School of Earth Science and Engineering, Xi'an Shiyou University, Xi'an 710065, P. R. China*

Complete contact information is available at: https://pubs.acs.org/10.1021/acsomega.3c07863

Notes

The authors declare no competing financial interest.

■ ACKNOWLEDGMENTS

This work was financially supported by the National Natural Science Foundation of China (51402220), the Key Project of the Hubei Education Department (D20191503), and the Wuhan Institute of Technology Science Foundation (K201801).

■ REFERENCES

(1) Wang, X.; Zhang, L.; Li, Z.; et al. Pore type classification scheme for continental Yanchang shale in Ordos Basin and its geological significance. *Oil Gas Geol.* **2016**, *37* (1), 1−7.
(2) Li, K.; Chunyu, W. A. N. G. Study on the matching relationship of solid grains to formation aperture. *Fault-Block Oil Gas Field* **2000**, *7* (5), 24−25.
(3) Zhao, X.; Bai, Y.; Wang, Z.; et al. Summary about application of emulsion system in oilfield. *Sino-Global Energy/Zhongwai Nengyuan* **2011**, *16* (11), 45−50.
(4) Zhou, W.; Lu, Y.; Gao, C.; et al. Effects of flow pattern and pore size on immiscible continuous three-phase displacement. *Energy Fuels* **2013**, *27* (2), 717−724.
(5) Chaudhury, M. K. Complex fluids: Spread the word about nanofluids. *Nature* **2003**, *423* (6936), 131−132.

(6) Wasan, D. T.; Nikolov, A. D. Spreading of nanofluids on solids. *Nature* **2003**, *423* (6936), 156−159.
(7) Bernard, G. G. *Effect of floodwater salinity on recovery of oil from cores containing clays*, SPE California Regional Meeting, SPE-1725-MS: Los Angeles, California, 1967.
(8) Liu, K. L.; Kondiparty, K.; Nikolov, A. D.; et al. Dynamic spreading of nanofluids on solids part II: modeling. *Langmuir* **2012**, *28* (47), 16274−16284.
(9) Liq, Z.; Pu, W. F.; Wei, B.; et al. Static adsorption and dynamic retention of an anti - salinity polymer in low permeability sandstone core. *J. Appl. Polym. Sci.* **2017**, *134* (8), 113−116.
(10) Binks, B. P.; Rodrigues, J. A. Inversion of emulsions stabilized solely by ionizable nanoparticles. *Angew. Chem., Int. Ed.* **2005**, *44* (3), 441−444.
(11) Wei, B.; Li, Q.; Jin, F.; et al. The potential of a novel nanofluid in enhancing oil recovery. *Energy Fuels* **2016**, *30* (4), 2882−2891.
(12) Roustaei, A.; Bagherzadeh, H. Experimental investigation of SiO2 nanoparticles on enhanced oil recovery of carbonate reservoirs. *J. Pet. Explor. Prod. Technol.* **2015**, *5* (1), 27−33.
(13) Fan, H.; Striolo, A. Nanoparticle effects on the water-oil interfacial tension. *Phys. Rev. E* **2012**, *86* (5), No. 051610.
(14) Moghaddam, R. N.; Bahramian, A.; Fakhroueian, Z.; et al. Comparative study of using nanoparticles for enhanced oil recovery: Wettability alteration of carbonate rocks. *Energy Fuels* **2015**, *29* (4), 2111−2119.
(15) Zhao, M.; Lv, W.; Li, Y.; et al. Study on the synergy between silica nanoparticles and surfactants for enhanced oil recovery during spontaneous imbibition. *J. Mol. Liq.* **2018**, *26*, 373−378.
(16) Karimi, A.; Fakhroueian, Z.; Bahramian, A.; et al. Wettability alteration in carbonates using zirconium oxide nanofluids: EOR implications. *Energy Fuels* **2012**, *26*, 1028−1036.
(17) Taborda, E. A.; Franco, C. A.; Lopera, S. H.; et al. Effect of surface acidity of SiO2 nanoparticles on thermal stability of polymer solutions for application in EOR processes. *J. Pet. Sci. Eng.* **2021**, *196*, No. 107802.
(18) Hassan, Y. M.; Guan, B. H.; Chuan, L. K.; et al. Interfacial tension and wettability of hybridized ZnOFe2O3/SiO2 based nanofluid under electromagnetic field inducement. *J. Pet. Sci. Eng.* **2022**, *221*, No. 110184.
(19) Yekeen, N.; Malik, A. A.; Idris, A. K.; et al. Foaming properties, wettability alteration and interfacial tension reduction by saponin extracted from soapnut (*Sapindus mukorossi*) at room and reservoir conditions. *J. Pet. Sci. Eng.* **2020**, *195*, No. 107591.
(20) Nowrouzi, I.; Manshad, A. K.; Mohammadi, A. H. Effects of dissolved carbon dioxide and ions in water on the dynamic interfacial tension of water and oil in the process of carbonated smart water injection into oil reservoirs. *Fuel* **2019**, *243*, 569−578.
(21) Ali, J. A.; Kolo, K.; Manshad, A. K.; et al. Recent advances in application of nanotechnology in chemical enhanced oil recovery: Effects of nanoparticles on wettability alteration, interfacial tension reduction, and flooding. *Egypt. J. Pet.* **2018**, *27* (4), 1371−1383.
(22) Nowrouzi, I.; Manshad, A. K.; Mohammadi, A. H. Effects of ions and dissolved carbon dioxide in brine on wettability alteration, contact angle and oil production in smart water and carbonated smart water injection processes in carbonate oil reservoirs. *Fuel* **2019**, *235*, 1039−1051.
(23) Esene, C.; Rezaei, N.; Aborig, A.; et al. Comprehensive review of carbonated water injection for enhanced oil recovery. *Fuel* **2019**, *237*, 1086−1107.
(24) Luo, D.; Wang, F.; Zhu, J.; et al. Nanofluid of graphene- based amphiphilic Janus nanosheets for tertiary or enhanced oil recovery: High performance at low concentration. *Proc. Natl. Acad. Sci. U.S.A.* **2016**, *113* (28), 7711−7716.

https://doi.org/10.1021/acsomega.3c07863
ACS Omega 2024, 9, 19043−19050